

## Reference

1. Fehse W. Automated Rendezvous and Docking of Spacecraft // Cambridge University Press. – 2003. 2. Manned space flights // CSRIeng - Bulletin of the news and analysis – 2013, № 19. 3. Norgia M., Giuliani G., Donati S. Absolute Distance Measurement With Improved Accuracy Using Laser Diode Self-Mixing Interferometry in a Closed Loop // IEEE

Transactions of Instr. & Measurement. – 2007, Vol. 56. 4. Zimpfer D., Kachmar P., Tuohy S. Autonomous rendezvous, capture and in-space assembly: Past, present, and future // 1st Space Exploration Conference: Continuing the Voyage of Discovery, Jan. – 2005.

Submitted on 25.11.13

С. Мартиш, д-р фіз.-мат. наук, Київський національний університет імені Тараса Шевченка  
В.Яценко, д-р техн. наук, Інститут космічних досліджень НАН та НКА України

### СИСТЕМИ З АКТИВНИМИ ІЧ-МАРКЕРАМИ ДЛЯ АВТОМАТИЧНОГО СТИКУВАННЯ КОСМІЧНИХ АПАРАТІВ

Для обслуговування супутників на орбіті вимагається здатності до зближення і стикування з допомогою безпілотних космічних апаратів, з відсутністю або мінімальним втручанням людини. Майбутні експедиції з дослідження космосу будуть покладатися на "інтелектуальні" автономні устаткування, для яких потрібні дуже складні системи технічного зору. Поява нових алгоритмів комп'ютерного зору і активних маркерів призведе до нового покоління систем зближення і стикування в найближчому майбутньому. Такі системи будуть здатні автономно виявляти цільовий супутник на старті останніх етапів зближення, оцінювати його пеленг, віддаль та відносну орієнтацію при будь-якому освітленні і в будь-якому його положенні.

Ключові слова: зближення і стикування, маркерний технічний зір, активні маркери.

Е. Мартыш, д-р физ.-мат. наук, Киевский национальный университет имени Тараса Шевченко  
В. Яценко, д-р техн. наук, Институт космических исследований НАН и НКА Украины

### СИСТЕМЫ С АКТИВНЫМИ ИК-МАРКЕРАМИ ДЛЯ АВТОМАТИЧЕСКОЙ СТЫКОВКИ КОСМИЧЕСКИХ АППАРАТОВ

Для обслуживания спутников на орбите требуется способности к сближению и стыковке с помощью беспилотных космических аппаратов, с отсутствием или минимальным вмешательством человека. Будущие экспедиции по исследованию космоса будут полагаться на "интеллектуальные" автономные устройства, для которых требуются очень сложные системы технического зрения. Появление новых алгоритмов компьютерного зрения и активных маркеров приведет к новому поколению систем сближения и стыковки в ближайшем будущем. Такие системы будут способны автономно обнаруживать целевой спутник на старте последних этапов сближения, оценивать его пеленг, удаление и относительную ориентацию при любом освещении и в любом его положении.

Ключевые слова: сближение и стыковка, маркерное техническое зрение, активные маркеры.

UDK 535.326

S. Pud, post grad. Stud., M. Petrychuk, PhD, V. Kovalenko, Dr.Sci., Prof.  
Department Electrophysics, Faculty of Radiophysics,  
Taras Shevchenko National University of Kyiv

## INFLUENCE OF THE ELECTROLYTE ON TRANSPORT CHARACTERISTICS OF ION-SENSITIVE SILICON NANOWIRE FIELD EFFECT TRANSISTORS

We report on the effect of the electrolyte on transport properties of open-gated silicon nanowire (NW) field effect transistor (FET) biosensor studied using noise spectroscopy. Exposing the Si NW FET to the electrolyte solution affects the threshold voltage, because it shifts the potential of the top dielectric layer. Also electrolyte ions screen the effect of the gate dielectric traps on channel transport. NWs of different lengths were used to exclude contact effects and show consistency of the measurement.

Key Words: silicon nanowires, open-gate, noise spectroscopy, electrolyte, biosensor.

**Introduction.** Silicon nanowire field effect transistors (Si NW FETs) are promising structures for the development of new biosensors due to their property of directly translating [interactions with target molecules into readable signals [6], [5]. These structures are highly sensitive and selective and are capable of real-time response and label-free detection. However, there are several important challenges, such as the stability and reproducibility of the operation of such sensors in a liquid environment due to the property changes of the thin gate dielectric when exposed to an electrolyte for a long time [4]. In this contribution, noise spectroscopy was employed to characterize the performance of the Si NW FET biosensors with the electrolyte solution (working as a top gate of the NW FET structure) on top and also without it. The influence of the electrolyte on transport was studied by changes of the device transport and noise characteristics. The results show that the electrolyte solution not only influences the threshold voltage of the transistor, but also affects the charge state of the surface traps.

**Experimental Details.** Transport and noise properties were measured and analyzed in Si NW FETs with a width of 500nm and a variety of lengths from 2 to 16 $\mu$ m (Fig. 1A). The nanowires were produced on the basis of silicon-on-insulator (SOI) wafers using nanoimprint technology with subsequent wet chemical etching of the NW structures. The contacts to the NWs were highly As implanted, so the NW represented a FET with inverted n-type channel. The

NW sensors were protected from the electrolyte by a thin thermally grown SiO<sub>2</sub> passivation layer (10nm thickness). The measurements were performed with phosphate-buffered saline (PBS) electrolyte on top of the passivation layer of the NW FET structure and without electrolyte (in air) at different back-gate voltages, V<sub>G</sub>.

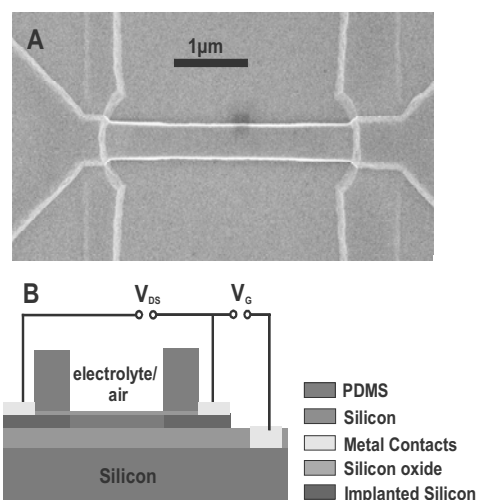


Fig. 1. (A) SEM image of a 500 nm wide silicon nanowire.  
(B) Sketch of the measurement set-up

The back-gate voltage,  $V_G$ , was applied to the substrate of the silicon-on-insulator (SOI) wafer. The schematic of the experiment is shown in Fig. 1B. The potential of the drain,  $V_{DS}$ , as well as the back gate,  $V_G$ , was set against the grounded source. In all experiments shown here,  $V_{DS}$ , was set to a value of 100 mV to maintain a linear regime of operation of the NW transistor. In this regime, the differential resistance of the sample equals the normal value of resistance, which makes it much simpler to evaluate the normalized current noise spectral density (NCNSD),  $S_I/I^2$ , using the measured drain voltage noise spectral density.

It should be noted that the noise spectra and the I-V curves were measured in a constant DC mode. The drain voltage,  $V_{DS}$ , and back-gate voltage,  $V_G$ , were applied using a battery loaded with the sample and a load resistance.

**Results and discussion.** The transfer characteristics of the Si NW transistors were measured in DC mode in air and in electrolyte (Fig. 2).

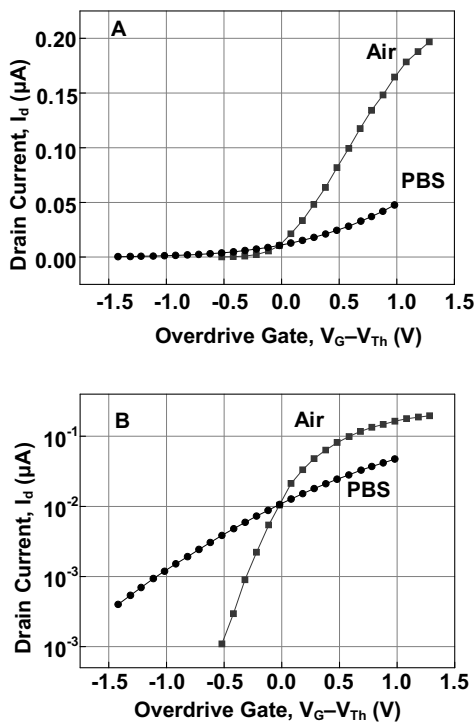


Fig. 2. Transfer curves of the 8µm Si NW FET measured in air (red curves) and in PBS (black curves) plotted on linear scale(A) and on logarithmic scale(B)

The measurement set-up was as described above. The drain current,  $I_d$ , controlled by the back-gate voltage is higher in air than in the electrolyte in overthreshold mode, at  $V_G > V_{Th}$  (Fig. 2A) and higher in electrolyte than in air in subthreshold mode,  $V_G < V_{Th}$ . It should be emphasized that each point of the transfer characteristics was measured at a stabilized drain current. After the back-gate voltage was applied, the drain current increased with time until it reached a certain saturation value. The time between applying the gate voltage and saturation of the drain current was around 20 min in the case of air and around one minute in the case of electrolyte. The leakage current through the back-gate electrode was negligibly small (below 0.1nA). Therefore we suggest that such an effect is related to charging of the traps located in the top dielectric layer through the back-gate electrode [2]. The time constant of such a process is so large because the traps are charged with extremely small currents through the back-gate dielectric. The decrease of the charging time in the electrolyte can be explained by the

effect of charge screening. In the presence of the electrolyte, the charge accumulated in the top passivation dielectric is immediately screened by the ions of the electrolyte solution. Therefore the conductivity of the channel changes much faster in the electrolyte, but the influence of the back gate on the channel through the charging of top dielectric layer decreases. The slope of the transfer curve is higher in air than in the PBS solution (Fig. 2A). And this difference can also be explained by charging the top dielectric layer through the back gate and the screening effect in the electrolyte. In the subthreshold region (Fig.2B), we can observe that the subthreshold current in the electrolyte is higher than in air.

As mentioned above, all measurements were performed at low drain voltages (100mV). In such a regime, the subthreshold current is not related to transport through surface states, but is mainly defined by diffusion [1]. The increase of the subthreshold current in PBS solution can again be explained by screening of the potential of the top dielectric layer by ions in the electrolyte. In the subthreshold mode, negative overdrive gate voltages are applied to the sample, and screening of the negative overdrive potentials by ions in the electrolyte means shifting the surface potential to zero, which, in turn, leads to an increasing drain current. The curves measured in air and in PBS solution coincide within the close vicinity of the zero overdrive gate voltage. This means that screening does not occur in this point and that the zero overdrive gate voltage is close to the flat-band point. Therefore we can conclude that introducing PBS on top of the NW transistor affects transport in the transistor through screening of the surface potential of the top dielectric layer [3].

Behavior similar to that described above is also registered in the samples with different channel lengths. The drain current with the same value of the overdrive gate voltage,  $V_G - V_{Th}$ , is plotted versus the channel length of the device in Fig.3.

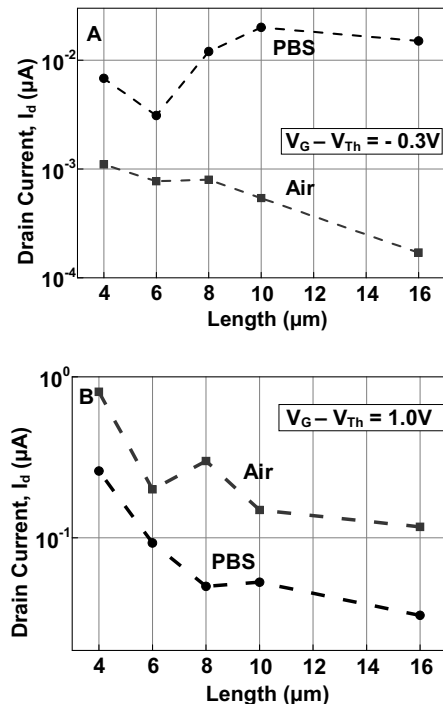


Fig. 3. Drain current through Si NW FETs measured in air (red curves) and in PBS (black curves) plotted versus channel length at drain voltage of 100 mV in subthreshold mode (A) and in overthreshold mode(B)

The drain current is well scaled with the length of the sample (Fig. 3A in air and Fig. 3B). Contact resistance

can be estimated from the dependence of the drain current on length by linear approximation (Fig. 3A in Air). The value obtained is in the range between 8 and 12 kOhm for different measured chips, which is much lower than the device channel resistance, even when it is opened. Only Si NWs with shorter channels (4 and 6  $\mu\text{m}$ ) are affected by the contact resistance (Fig. 3A in Air). In the case of the PBS solution on the surface of the Si NW biosensor, the subthreshold current is higher than in air and vice versa – the overthreshold current in PBS is lower than in air. Subthreshold current in PBS (Fig. 3A) is no longer scaled with length. This may be due to the fact that the current in the subthreshold region is strongly affected by the electrolyte, which influences the surface potential of the gate dielectric.

The influence of PBS on transport in Si NW FET is also confirmed by noise measurements. Fig. 4 shows the normalized current noise spectral density (NCNSD),  $S_I/I^2$ , at subthreshold and overthreshold voltages measured in air and PBS. In the subthreshold region, NCNSD in the device decreased when PBS was introduced into the sample. This decrease can be partially explained by the changing of the subthreshold current. This current increased by a factor of 3 (Fig. 2b at an overdrive gate of -0.2V) after submerging a sample in PBS. Therefore, the NCNSD,  $S_I/I^2$ , has to decrease by approximately one order of magnitude, but from Fig. 4A we can see that the value of NCNSD is more than one order of magnitude lower in PBS compared to that as in air.

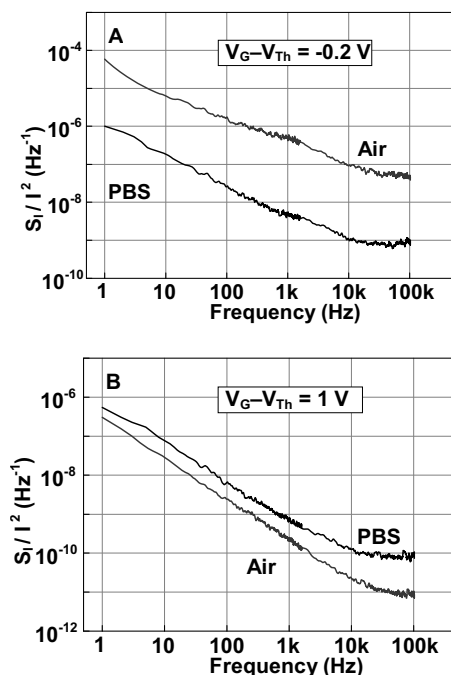


Fig. 4. Normalized current noise spectral density (NCNSD),  $S_I/I^2$ , at sub-threshold (A) and overthreshold (B) overdrive gate voltages measured in air (red curves) and PBS (black curves)

С. Пуд, асп., М. Петричук, канд. фіз.-мат. наук,  
В. Коваленко, д-р фіз.-мат. наук, проф.  
кафедра електрофізики, радіофізичний факультет,  
Київський національний університет імені Тараса Шевченка

### ВПЛИВ ЕЛЕКТРОЛІТУ НА ЕЛЕКТРОФІЗИЧНІ ХАРАКТЕРИСТИКИ ІОННО-ЧУТЛИВИХ ПОЛЬОВИХ ТРАНЗИСТОРІВ НА БАЗІ КРЕМНІЄВИХ НАНОНИТОК

Досліджено вплив електроліту на електрофізичні властивості іонно-чутливих польових транзисторів на базі кремнієвих нанониток за допомогою шумової спектроскопії. Занурення польового транзистора на базі кремнієвих нанониток в розчин електроліту призводить до зсуву порогової напруги транзистора завдяки зміні потенціалу верхнього шару діелектрику. Також іони електроліту екранують вплив пасток верхнього шару діелектрику на транспорт в каналі транзистора. Для виключення контактних ефектів та підтвердження достовірності експерименту було проведено вимірювання транзисторів з різною довжиною каналу.

Ключові слова: кремнієві нанонитки, відкритий затвор, шумова спектроскопія, електроліт, біосенсор.

This is possible only if the exchange between the Si NW channel and the traps in the gate dielectric is affected. Thus, this decrease of NCNSD can be explained by the changing of the surface charge state in the sample's top dielectric due to PBS electrolyte adsorption and the screening effect as well as only a partial contribution of the increased subthreshold current. In the region above the threshold, submerging the sample in PBS results in a small increase in the amplitude of fluctuations in the sample. The lower value of the current at  $V_G - V_{Th} = 1.0$  V in PBS only partially influences the normalized noise level behavior.

The difference in NCNSD cannot be explained only by the difference in current. In this case, the current in air is approximately 3.25 times higher than in PBS (Fig. 2A), which means that without any other factors NCNSD should be at least an order of magnitude lower than in PBS. Our results show that exposing the nanowire samples to PBS in overthreshold mode decreases NCNSD only slightly. Therefore as in subthreshold mode, the overall excess noise in the Si NW channel is lower when we expose it to the electrolyte, in spite of the fact that the transconductance is lower in PBS than in air.

**Conclusion.** Transport properties of silicon nanowire field effect transistors exposed to air and to the electrolyte solution were investigated and compared utilizing noise spectroscopy. The results were obtained under quasistatic conditions in DC mode. It has been shown that the submerging of the nanowire samples in PBS affects the current in the NW channel by screening the charges, which accumulate in the top dielectric layer due to coupling between back and front gate. The investigated nanowire structures show good reproducibility in parameters. The devices of different lengths show similar behavior with the electrolyte and air on top. The produced Si NW FETs are well scaled with length and have contact resistance in the range of 10 kOhms, which is much lower than channel resistance. The noise measurements show that the electrolyte influences transport properties in the Si NW channel not only by screening surface potential, but it may also change the charge state of the traps in the top dielectric layer. As a result of such influence, the value of the excess noise is much lower in PBS than in air in the subthreshold region.

#### Reference

1. Chang J., Abidi A.A., Viswanathan C.R. Flicker noise in CMOS Transistors from Subthreshold to Strong Inversion at Various Temperatures // IEEE Trans. Electron Devices. – 1994. – N 11(41). – P. 1965–1971.
2. Hyung-Kyu L., Fossum J.G. Threshold Voltage of Thin-Film Silicon-on-Insulator (SOI) MOSFET's // IEEE Trans. Electron Devices. – 1983. – N ED-30(10). – P. 1244–1251.
3. Nair P.R., Alam M.A. Screening-limited response of nanobiosensors // Nanolett. – 2008. – N 8(5). – P. 1281–1285.
4. Nair P.R., Alam M.A. Design considerations of silicon nanowire biosensors // IEEE Trans. El. Dev. vol. 54, no. 12, pp. 3400–3408, 2007.
5. Patolsky F., Zheng G., Lieber C.M. Nanowire-based biosensors // Analytical Chemistry. – 2006. – N 78(13). – P. 4260–4269.
6. Ramgir N.S., Yang Y., Zacharias M. Nanowire-based sensors // Small. – 2010. – N 6(16). – P. 1705–1722.

Submitted on 19.09.13

С. Пуд, асп., М. Петричук, канд. физ.-мат. наук,  
В. Коваленко, д-р физ.-мат. наук, проф.  
кафедра электрофизики, радиофизический факультет,  
Киевский национальный университет имени Тараса Шевченко

### ВЛИЯНИЕ ЭЛЕКТРОЛИТА НА ЭЛЕКТРОФИЗИЧЕСКИЕ ХАРАКТЕРИСТИКИ ИОННО-ЧУВСТВИТЕЛЬНЫХ ПОЛЕВЫХ ТРАНЗИСТОРОВ НА БАЗЕ КРЕМНИЕВЫХ НАНОНИТЕЙ

Исследовано влияние электролита на электрофизические свойства ионно-чувствительных полевых транзисторов на базе кремниевых нанонитей с помощью шумовой спектроскопии. Погружение полевого транзистора на базе кремниевых нанонитей в раствор электролита приводит к смещению порогового напряжения транзистора благодаря изменению потенциала верхнего слоя диэлектрика. Также ионы электролита экранируют влияние ловушек верхнего слоя диэлектрика на транспорт в канале транзистора. Для исключения контактных эффектов и подтверждения достоверности эксперимента были проведены измерения транзисторов с различной длиной канала.

Ключевые слова: кремниевые нанонити, открытый затвор, шумовая спектроскопия, электролит, биосенсор.

UDC 681.785.3 (0.45)

A. Skrypets, Ph.D., V. Tronko, Dr. Sci,  
Avionics Department, Institute of Airnavigation, National Aviation University, Kyiv  
M. Asanov, Ph.D., Energy Supply and Physics Department,  
National Academy of Environmental Protection and Resort Development, Simferopol

### REMOTE MEASUREMENT OF POLARIZED RADIATION PARAMETERS

In this work a method for measuring the polarized radiation parameters by determining its ellipticity angle and azimuth of polarization ellipse is describes. It is proposed to additionally mechanically modulate the polarization plane of the analyzed radiation, pre-calculating the modulation amplitude. This method allows measuring relative Stokes vector components of radiation with highly accuracy in the entire optical range.

Keywords: polarized radiation, Stokes vector components, remote measurement

**Introduction.** Polarization is a fundamental physical characteristic of the radiation, which is conditioned by electromagnetic nature of light. Its measurement, followed by a theoretical analysis is a powerful diagnostic tool. The polarization state of light carries information not just about the characteristics of separate particles but also about the surface of the objects. Polarization methods of analysis have been used particularly in medicine [1, 2, 5], during studying material surface [4], in aerospace remote sensing [3, 8]. Increasing the accuracy of determining the Stokes vector components of the polarized radiation is an important and urgent problem.

In [6] authors proposed a photopolarimetric method for determining the polarized radiation parameters. The basis of this method is the measurement of the ellipticity angle and the azimuth of the polarization ellipse of optical radiation by Stokes polarimeter with the modulation of the polarization plane of analyzed radiation by Faraday cell. The active element of a Faraday cell is transparent in the near-infrared range yttrium iron garnet. Additional modulation of the polarization plane of the radiation increased the accuracy of the ellipticity angle and the azimuth of the polarization ellipse measurement, and, consequently, the relative values of the Stokes vector components. However, using the yttrium iron garnet as an active element of Faraday cell limits the application of the proposed Stokes polarimeter by IR range. Additionally, the domain structure of yttrium iron garnet partially depolarizes passing light radiation that reduces the accuracy of the determination of the Stokes vector components.

In this work the Stokes polarimeter is described, in which instead of a magneto-optical Faraday cell is proposed to use a mechanical modulation of the polarization plane. This Stokes polarimeter will allow to provide studies of radiation in the entire optical range without significantly reducing the accuracy and sensitivity of measurements.

**Description.** Block diagram of proposed Stokes polarimeter is shown in Fig. 1. To determine the azimuth of the polarization ellipse  $\lambda$  and the ellipticity angle  $\omega$  one needs to make two measurements.

While measuring the azimuth of the polarization ellipse  $\lambda$  the most transmission plane azimuths of analyzers 1 and 2 are set to  $\beta - \theta$  and  $\beta + \theta$  angles respectively

(Fig. 1, a). The angle  $\theta$  is pre-calculated so that the signal-to-noise ratio at the output of photodetector was maximal [7]. The switch 5 converts the voltage into an alternating electric signal by passing signals in turn from the two photodetectors 3 and 4.

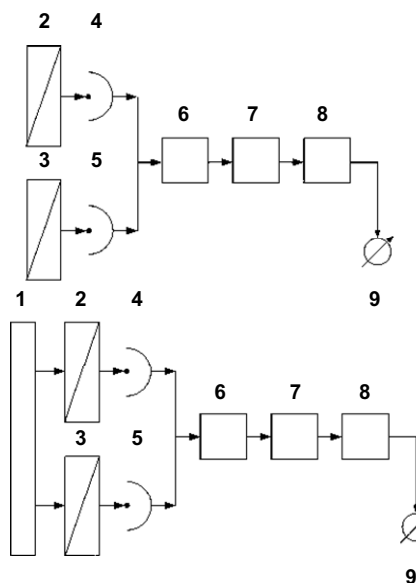


Fig. 1. Block diagram of Stokes polarimeter:  
1 –  $\lambda/4$  phase plate; 2, 3 – analyzers; 4, 5 – photodetectors;  
6 – switch; 7 – amplifier; 8 – synchronous detector;  
9 – ammeter (indicator)

Intensities of radiation at the output of the analyzers will be given by:

$$I_{OUT_2} = \frac{I}{2}(k_1 + k_2) \times [1 + (1 - 2Gd) p \cos 2\omega \cos 2(\lambda - \beta + \theta)] ;$$

$$I_{OUT_3} = \frac{I}{2}(k_1 + k_2) \times [1 + (1 - 2Gd) p \cos 2\omega \cos 2(\lambda - \beta - \theta)] ,$$

where  $I$  is the total intensity of the incident radiation;  $k_1$ ,  $k_2$  are the principle transmittances of polarizing prisms;  $Gd$  is polarization defect of prism,  $p$  is the polarization degree of the analyzed radiation.